E-field control of magnetization and susceptibility of AFE-based YIG/PLZST heterostructure

Liuyang Han, Freddy Ponchel, Denis Remiens, Tuami Lasri, Nicolas Tiercelin, Philippe Pernod, Genshui Wang

E-field control of magnetization and susceptibility of AFE-based YIG/PLZST heterostructure

Liuyang Han[a,b,c], Freddy Ponchel[a], Denis Rémiens[a] , Tuami Lasri[a], Nicolas Tiercelin[a], Philippe Pernod[a], Genshui Wang[b]

a-Univ. Polytechnique Hauts-de-France, CNRS, Centrale Lille, ISEN, Univ. Lille, UMR 8520-IEMN, Joint International Laboratory LIA LICS/LEMAC, F-59000, Lille, France
b-Key Laboratory of Inorganic Functional Materials and Devices and State Key Laboratory of High Performance Ceramics and Superfine Microstructure, Shanghai Institute of Ceramics, Chinese Academy of Sciences, Shanghai, 200050, People's Republic of China
c-University of Chinese Academy of Sciences, Beijing, 100049, People's Republic of China

Abstract
The magnetoelectric properties of a laminated heterostructure consisting of ferromagnetic yttrium iron garnet (YIG) film and antiferroelectric $(Pb_{0.97}La_{0.02})$ $(Zr_{0.6}Sn_{0.3}Ti_{0.1})O_3$ (PLZST) ceramic is, for the first time, reported in this work. The electric-field-controlled susceptibility, a shift of the coercive magnetic field and magnetization variations are demonstrated in YIG/PLZST multiferroic heterostructure. A large variation of the relative magnetic susceptibility is observed, practically 33% at a low magnetic field of 10 Oe. A sharp reduction of magnetization occurs at the antiferroelectric-ferroelectric phase transition field of PLZST ceramic. Thus the converse magnetoelectric coefficient peaks at the switching field and the maximum can reach 11.6×10^{-8} s/m without bias magnetic field. These features indicate that antiferroelectric materials can also be alternative candidates to combine with ferromagnetic materials for magnetoelectric tunable devices.

1. Introduction

Multiferroic composite materials, with two or more ferroic (ferro-electric, ferro/ferrimagnetic, ferroelastic) phases [1–3], have offered a great potential and opportunities in developing novel multifunctional devices, such as memory devices, sensors, phase shifters, transducers, filters, oscillators, etc. [4–7]. Nevertheless, investigations for a better understanding of fundamental physics and engineering potential of these materials and structures are still on the way.

Previous researchers have studied a variety of layered magneto-electric (ME) heterostructures of ferromagnetic (FM) and ferroelectric (FE) components [8–10]. Actually, the main interest has been focused on FM/FE heterostructures and in particular the electric-field tuning of the magnetic response resulting from the strain of FE component transferred to FM component, the so-called converse ME effect (CME). As antiferroelectric (AFE) materials enjoy a large strain change during the electric-field induced AFE-FE transition and display zero polarization and strain in a relaxed state [11,12], there are potential benefits for their use. The high electric-field induced phase transition strain makes that AFE-based ME composites are also interesting and can yield a good tuning of the magnetic response with electric field. Another advantage is that the non-remnant state results in no pre-poling process, which is a very important point from an application point of view [13]. The electric-field control of magnetism in AFE-based composites has been rarely demonstrated, and the reported works are mainly focused on microwave frequency ME coupling effect [14,15]. A comprehensive research on E-field controlled magnetism at static magnetic state is necessary in AFE-based ME heterostructure.

Yttrium iron garnet (YIG) is considered to be a good choice for the magnetic material when targeting tunable multiferroic microwave de-vices thanks to its outstanding advantages including small magneto-crystalline anisotropy, narrow ferromagnetic resonance line width, high resistivity, and low microwave losses. Therefore, most of the works are focused on ME interactions of YIG/FE at microwave frequencies (mainly X-band). The voltage tuning of ferromagnetic resonance (FMR) field in composites made of a YIG film and different FE layers has been widely reported, while the electric field tuning of magnetism at static state is rarely investigated. To understand the CME coupling effect, it is necessary to study the electric-field tuning of magnetism of YIG at static state [16]. Lian et al. have firstly reported the voltage-controlled magnetization of YIG/FE multiferroic heterostructure with DC magnetic field

[17]. The study of E-field tuning of magnetism, not at microwave frequency but at static state, in YIG/AFE heterostructure has not been reported yet, to the best of the authors' knowledge.

This work is dedicated to the study of a layered multiferroic structure consisting of the ferromagnetic YIG film and an AFE ceramic inserted between platinum (Pt) electrodes. The $Pb_{0.97}La_{0.02}Zr_{0.6}Sn_{0.3}Ti_{0.1}O_3$ (PLZST) ceramic, a typical AFE material [18], is selected to be the AFE substrate for its sharp E-field induced phase transition strain change. A significant tuning of the magnetic response has been achieved at static state (DC electric field and bias DC magnetic field) in this unique FM–AFE heterostructure. The voltage control of the magnetic susceptibility and the magnetization has been demonstrated and the CME coefficient has been evaluated. The results indicate the AFE ceramics can also be potential candidates as the strain-offer layer in the ME coupling composites.

2. Experimental

The multiferroic composites are designed to be layered structures of YIG film and PLZST AFE ceramics with Pt electrodes. The PLZST ceramics were fabricated by the conventional solid state reaction, and the sintered ceramics were machined and fine polished into $10 \times 10 \times 0.5$ mm^3 substrates, as given in Ref. [19]. Then the Pt electrodes were deposited on the two sides of the PLZST ceramic by magnetron sputtering with a thickness of 80 nm. The YIG film was deposited on one side of Pt/PLZST/Pt structure by radio-frequency magnetron sputtering in a thickness of 400 nm. The deposition conditions and annealing process of YIG film have been presented in Ref. [17]. The dimensions of the ceramic substrate and Pt electrodes are respectively 10×10 mm^2 and 6×6 mm^2, while the YIG film is 5×3 mm^2. The X-ray diffraction (XRD) of YIG/Pt/PLZST/Pt was performed using a Rigaku D x-ray diffractometer and the scanning electron microscopy (SEM) was employed to characterize the interface of the heterostructure. The electric hysteresis loop (P-E) and the field-induced strain curve (S-E) of the PLZST were obtained with a standard ferro-electric tester (TF analyzer 2000, aixACCT, Germany). The magnetic hysteresis loops ((M−H)) with different electric fields and the electric field tuning of magnetization (M-E) were measured at room temperature by a Vibration Sample Magnetometer (VSM, ADE model EV9) combined with an external DC voltage supply (SPS Model PS350), as described in Ref. [19]. The sample was placed in the VSM system with two copper wires soldered with electrodes. Thus, it was possible to apply a magnetic field as well as an electric field to the sample simultaneously. To ensure the measurements accuracy a calibration of the measurements was performed by taking into account the influence of the PLZST, Pt electrodes, wires and so on (de-embedding technique).

3. Results and discussion

The Fig. 1(a) shows the P-E loop and the I-E curve while the Fig. 1(b) describes the S-E curve of PLZST ceramic. The AFE characteristics of double P-E loop, four current peaks and horn-like S-E curve are clearly observed in PLZST. The polarization and strain are nearly zero when the electric field is lower than the switching field. The zero-remnant state makes AFE materials free from the influence of the electric load history and eliminates the pre-poling process that is necessary for FE materials. The switching fields of AFE-FE phase transition are 50 kV/cm and 25 kV/cm, and the maximum strain can reach 0.2%. The sharp strain change generated by the electric-field-induced structure phase transition gives us possibilities to obtain in-plane strain-mediated magnetism transformation via the electric field application.

The schematic of YIG/Pt/PLZST/Pt ME heterostructure with electric and magnetic fields together with the cross-sectional SEM picture are given in Fig. 1(c). The PLZST ceramic substrate is polycrystalline, it exhibits isotropic in-plane strain when the electric field is perpendicular to the plane. The YIG film being polycrystalline it demonstrates iso-tropic in-plane magnetic properties, thus the magnetic field direction is parallel to the substrate plane. The interface is clear, indicating no significant diffusion between the film and the ceramic substrate. The XRD pattern of YIG/Pt/PLZST/Pt heterostructure is illustrated in Fig. 1(d). The peaks of YIG film, Pt electrode and PLZST ceramic are well observed on the XRD pattern. The peak intensity of YIG film is much weaker than PLZST ceramic because of its

low thickness. All of these peaks belong to cubic $Y_3Fe_5O_{12}$ phase, and there are no other phases that appear up to the detection limit.

We have measured the magnetization variations M ($M = M_E - M_0$) while applying an electric field across the PLZST ceramic in order to investigate the ME coupling in a static magnetic state. The initial magnetization (M_0) is defined as the magnetization without electric field and M_E is the magnetization for E. The relative magnetization change (M/M_0) is generated in response to the application of an electric field, and the M/M_0-E curve at 0 Oe is given as a representative in Fig. 2(a). The horn-like shape M/M_0-E curve was found to be similar to the strain-field curve in Fig. 1(b), suggesting a strong strain-driven magnetization change in YIG/Pt/PLZST/Pt heterostructure. The CME coefficient (α_{CME}) at 0 Oe, calculated from the equation: $\alpha_{CME} = \mu_0 \delta M/\delta E$ ($\mu_0 = 4\pi \times 10^{-7}$ H/m), is also given in Fig. 2(a). It is observed that, because of the sharp strain change at the forward and backward switching fields of PLZST ceramic, the α_{CME} peaks at four switching fields. The maximum value recorded is 11.6×10^{-8} s/m.

To explore the influence of the bias magnetic field on the CME effect, the maximums of M/M_0 and α_{CME} for three different bias magnetic fields (0, 15, 30 Oe) are reported in Fig. 2(b). It is worth noting that the maxima for both, M_{max}/M_0 and α_{max}, are obtained with a bias magnetic field of 0 Oe. The fact that the best performance of CME coupling can be obtained without magnetic field is an important asset in terms of design when targeting ME devices conception.

We have measured (M−H) loops of the heterostructure while an electric field is applied across the PLZST ceramic in order to investigate the ME coupling in a static electric state. The (M−H) loops with different electric fields and the H_C-E curve are given in Fig. 3(a) and (b), respectively. When the external electric field is lower than the AFE-FE switching field of PLZST, the (M−H) loops coincide with the one obtained without electric field. Once the electric field is higher than AFE-FE switching field, the remnant magnetization decreases sharply, and the (M−H) loops become difficult to be saturated. In this case, an induced magnetic coercive field shift is generated in response to the electric field application. The strain generated from the electric-field-induced AFE-FE phase transition is transferred through the Pt electrodes to the YIG film, which leads to magnetocrystalline anisotropy transformation in the YIG film.

The magnetic susceptibility (χ) versus magnetic field, (χ-H) curve, is shown in Fig. 4(a).The χ reaches a maximum at 20 Oe, near H_C. To observe the influence of the electric field strength on the YIG film susceptibility at a given magnetic field, the χ-E curve for a magnetic field of 10 Oe is presented in Fig. 4(b). It is noteworthy that the electric field facilitates a reduction in the susceptibility, which yields a maximum variation, as a function of the electric field, of $\chi = 13.5$ at 10 Oe. The maximum relative χ change reaches $\chi/\chi_0 = 33\%$ at 10 Oe. This change of χ gives rise to the tunability of the permeability and thus opens pathway towards the design of voltage tunable inductors.

Additionally, the H_C-E and χ-E curves clearly display the similar horn-like shape but the horns are in opposite directions, which is attributed to the correlation between the strain and the electric field. The shape of H_C-E and χ-E curves demonstrates the effective control of magnetocrystalline anisotropy transformation by E-field via strain mediated mechanism.

For comparison purposes, Table 1 summarizes important results measured at static magnetic state for different layered structures recently reported. It is found that this work is the first to demonstrate the relative magnetic susceptibility change in an AFE-based ME hetero-structure. Further, the CME coefficient is obtained without the application of bias magnetic field, which is a strong asset in terms of cost and ease of procedures. The high relative magnetic susceptibility change reveals a good opportunity for the development of ME tunable devices based on AFE materials

4. Conclusions

In summary, the E-field controlled magnetism in an AFE-based ME heterostructure of YIG/PLZST is reported for the first time. A comprehensive study of magnetization, magnetic coercive field, magnetic susceptibility and CME coefficient responses to an electric field is achieved in this work. The

electric field induced phase transition strain in an AFE substrate plays the key role in ME coupling and its unique zero-remnant state gives us the possibility to avoid pre-poling process. The maximum α_{CME} is 11.6×10^{-8} s/m without magnetic field, and the χ/χ_0 can reach 33% with a low magnetic field of 10 Oe. The large magnetic susceptibility variation capability given by this composite, YIG/Pt/PLZST/Pt, shows great potential for ME tunable devices.

Acknowledgements
This work was supported by the Ph.D. funding of Université Polytechnique Hauts-de-France, International Partnership Program of Chinese Academy of Sciences (Grant No. GJHZ1821), Chinese Academy of Sciences President's International Fellowship Initiative (Grant No. 2017VEA0002). The authors would like to thank Dr. Chenhong Xu for his generous assistance in the preparation of the ceramic.

References
[1] S.Fusil, V.Garcia, A.Barthélémy, M.Bibes, Magnetoelectric devices for spintronics, Annu. Rev. Mater. Res. 44 (2014) 91–116, https://doi.org/10.1146/annurev- matsci-070813-113315.
[2] M.Staruch, D.B.Gopman, Y.L.Iunin, R.D.Shull, S.F.Cheng, K.Bussmann, P.Finkel, Reversible strain control of magnetic anisotropy in magnetoelectric heterostructures at room temperature, Sci. Rep. 6 (2016), https://doi.org/10.1038/ srep37429.
[3] M. Atif, M. Nadeem, W. Khalid, Z. Ali, Structural, magnetic and impedance spectroscopy analysis of (0.7)CoFe2O4+(0.3)BaTiO3 magnetoelectric composite, Mater. Res. Bull. 107 (2018) 171–179, https://doi.org/10.1016/j.materresbull. 2018.07.026.
[4] A.B. Ustinov, G. Srinivasan, B.A. Kalinikos, Ferrite-ferroelectric hybrid wave phase shifters, Appl. Phys. Lett. 90 (2007) 031913, https://doi.org/10.1063/1.2432953.
[5] Y.K. Fetisov, G. Srinivasan, Electrically tunable ferrite-ferroelectric microwave delay lines, Appl. Phys. Lett. 87 (2005) 103502, https://doi.org/10.1063/1. 2037860.
[6] M.M. Vopson, Fundamentals of multiferroic materials and their possible applications, Crit. Rev. Solid State Mater. Sci. 40 (2015) 223–250, https://doi.org/10. 1080/10408436.2014.992584.
[7] S. Priya, R. Islam, S. Dong, D. Viehland, Recent advancements in magnetoelectric particulate and laminate composites, J. Electroceramics 19 (2007) 149–166, https://doi.org/10.1007/s10832-007-9042-5.
[8] M. Liu, Z. Zhou, T. Nan, B.M. Howe, G.J. Brown, N.X. Sun, Voltage tuning of ferromagnetic resonance with bistable magnetization switching in energy-efficient magnetoelectric composites, Adv. Mater. 25 (2013) 1435–1439, https://doi.org/10. 1002/adma.201203792.
[9] A.D. Sheikh, V.L. Mathe, Composition dependent phase connectivity, dielectric and magnetoelectric properties of magnetoelectric composites with Pb(Mg1/3Nb2/3) 0.67Ti0.33O3 as piezoelectric phase, Mater. Res. Bull. 44 (2009) 2194–2200, https://doi.org/10.1016/j.materresbull.2009.08.008.
[10] A.S. Tatarenko, V. Gheevarughese, G. Srinivasan, O.V. Antonenkov, M.I. Bichurin, Microwave magnetoelectric effects in ferrite—piezoelectric composites and dual electric and magnetic field tunable filters, J. Electroceramics 24 (2010) 5–9, https://doi.org/10.1007/s10832-007-9382-1.
[11] S. Lepadatu, M. Vopson, S. Lepadatu, M.M. Vopson, Heat-assisted multiferroic solid- state memory, Materials 10 (2017) 991, https://doi.org/10.3390/ma10090991.
[12] X. Hao, J. Zhai, L.B. Kong, Z. Xu, A comprehensive review on the progress of lead zirconate-based antiferroelectric materials, Prog. Mater. Sci. 63 (2014) 1–57, https://doi.org/10.1016/j.pmatsci.2014.01.002.
[13] Z. Zhou, Q. Yang, M. Liu, Z. Zhang, X. Zhang, D. Sun, T. Nan, N. Sun, X. Chen, Antiferroelectric materials, applications and recent progress on multiferroic heterostructures, SPIN 5 (2015) 1530001, , https://doi.org/10.1142/ S2010324715300017.
[14] Z. Zhou, X.Y. Zhang, T.F. Xie, T.X. Nan, Y. Gao, X. Yang, X.J. Wang, X.Y. He, P.S. Qiu, N.X. Sun, D.Z. Sun, Strong non-volatile voltage control of magnetism in magnetic/antiferroelectric magnetoelectric heterostructures, Appl. Phys. Lett. 104 (2014) 012905, https://doi.org/10.1063/1.4861462.

[15] J.-P. Zhou, X.-Z. Chen, L. Lv, C. Liu, P. Liu, Magnetoelectric coupling in antiferro- electric and magnetic laminate composites, Appl. Phys. A 104 (2011) 461–464, https://doi.org/10.1007/s00339-011-6261-z.
[16] J. Lian, F. Ponchel, N. Tiercelin, Y. Chen, D. Rémiens, T. Lasri, G. Wang, P. Pernod, W. Zhang, X. Dong, Electric field tuning of magnetism in heterostructure of yttrium iron garnet film/lead magnesium niobate-lead zirconate titanate ceramic, Appl. Phys. Lett. 112 (2018) 162904, , https://doi.org/10.1063/1.5023885.
[17] J. Lian, F. Ponchel, N. Tiercelin, L. Han, Y. Chen, D. Rémiens, T. Lasri, G. Wang, P. Pernod, W. Zhang, X. Dong, Influence of the magnetic state on the voltage- controlled magnetoelectric effect in a multiferroic artificial heterostructure YIG/ PMN-PZT, J. Appl. Phys. 124 (2018) 064101, , https://doi.org/10.1063/1. 5037057.
[18] M. Chen, X. Yao, L. Zhang, Preparation of (Pb, La)(Zr, Sn, Ti)O3 antiferroelectric ceramics using colloidal processing and the field induced strain properties, J. Eur. Ceram. Soc. 21 (2001) 1159–1164, https://doi.org/10.1016/S0955-2219(00) 00336-8.
[19] L. Han, F. Ponchel, N. Tiercelin, D. Rémiens, T. Lasri, P. Pernod, G. Wang, Electric field tuning of magnetization in an antiferroelectric-based heterostructure: example of NMG/PLZST/NMG, J. Am. Ceram. Soc. 102 (2019) 3809–3813, https://doi.org/ 10.1111/jace.16356.
[20] C. Thiele, K. Dörr, O. Bilani, J. Rödel, L. Schultz, Influence of strain on the mag- netization and magnetoelectric effect in La 0.7 A 0.3 Mn O 3 ⁄ PMN − PT (001) (A = Sr, Ca), Phys. Rev. B 75 (2007), https://doi.org/10.1103/PhysRevB.75.054408.
[21] J.J. Yang, Y.G. Zhao, H.F. Tian, L.B. Luo, H.Y. Zhang, Y.J. He, H.S. Luo, Electric field manipulation of magnetization at room temperature in multiferroic CoFe2O4/ Pb(Mg1/3Nb2/3)0.7Ti0.3O3 heterostructures, Appl. Phys. Lett. 94 (2009) 212504, https://doi.org/10.1063/1.3143622.
[22] S. Zhang, Y.G. Zhao, P.S. Li, J.J. Yang, S. Rizwan, J.X. Zhang, J. Seidel, T.L. Qu, Y.J. Yang, Z.L. Luo, Q. He, T. Zou, Q.P. Chen, J.W. Wang, L.F. Yang, Y. Sun, Y.Z. Wu, X. Xiao, X.F. Jin, J. Huang, C. Gao, X.F. Han, R. Ramesh, Electric-field control of nonvolatile magnetization in Co 40 Fe 40 B 20 / Pb (Mg 1 / 3 Nb 2 / 3) 0.7 Ti 0.3 O 3 structure at room temperature, Phys. Rev. Lett. 108 (2012), https:// doi.org/10.1103/PhysRevLett.108.137203.

Table 1
Summary of ME coupling parameters for some laminated structures.

Structure	α_{CME} ($\times 10^{-8}$ s/m)	M/M	bias H (Oe)	χ/χ_0
YIG/PLZST (this work)	11.6	18.4%	0	32.7% @10 Oe
YIG/$Pb(Mg_{1/3}Nb_{2/3})O_3$-$Pb(Zr,Ti)O_3$ [17]	10.9	7%	40	16.8% @30 Oe
$La_{0.7}Sr_{0.3}MnO_3$//$Pb(Mg_{1/3}Nb_{2/3})O_3$-$PbTiO_3$(001) [20]	6	25%	100	–
$CoFe_2O_4$//$Pb(Mg_{1/3}Nb_{2/3})O_3$- $PbTiO_3$ (001) [21]	3.2	6%	500	–
$Co_{40}Fe_{40}B_{20}$/ /$Pb(Mg_{1/3}Nb_{2/3})O_3$- $PbTiO_3$ (001) [22]	200	17.6%	5	–

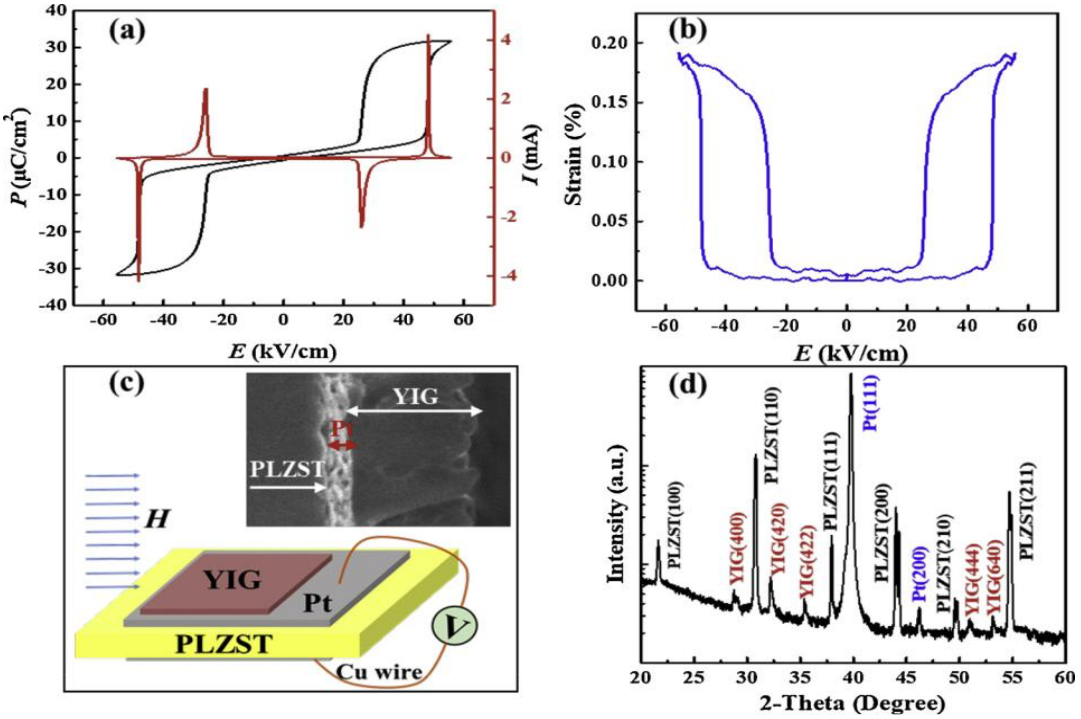

Fig. 1. (a) P-E loop, I-E curve and (b) S-E curve of PLZST ceramic substrate, (c) schematic and inset the cross-sectional SEM picture of YIG/Pt/PLZST/Pt ME heterostructure, (d) XRD pattern of YIG/Pt/PLZST/Pt heterostructure.

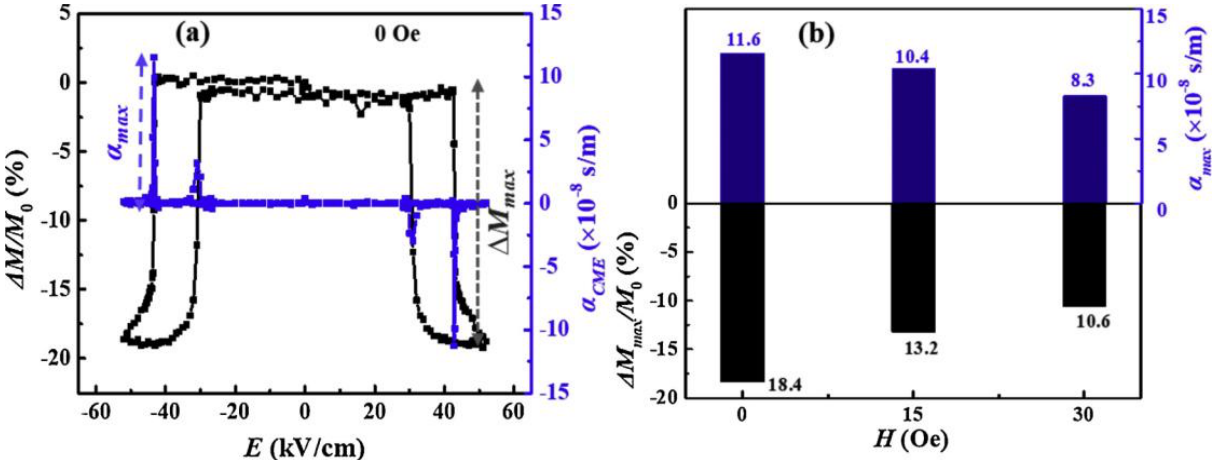

Fig. 2. (a) M/M_0-E and α_{CME}-E curves at 0 Oe and (b) M_{max}/M_0-H and αmax-H bar charts of YIG/Pt/PLZST/Pt heterostructure

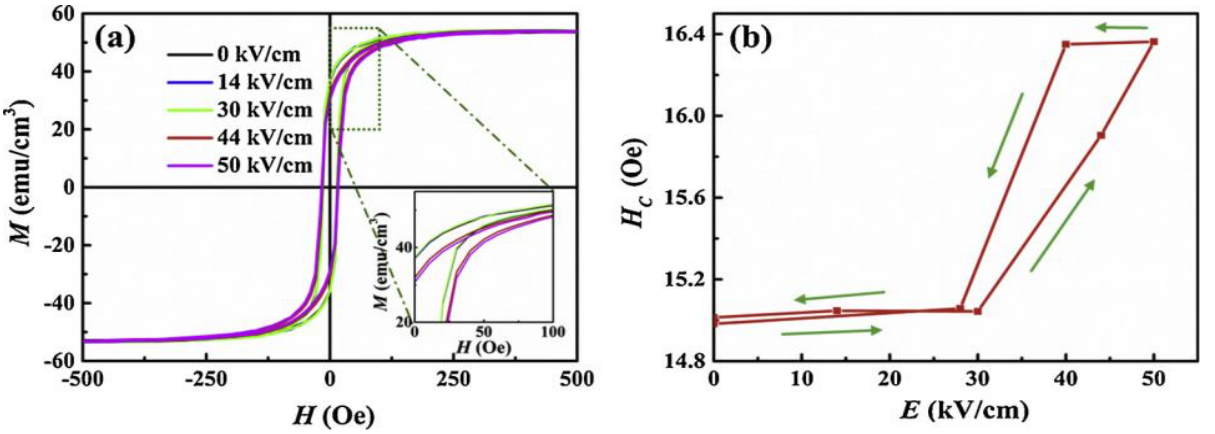

Fig. 3. (a) (M−H) loops, inset the enlarged (M−H) loops, (b) H_C-E curve of YIG/Pt/PLZST/Pt heterostructure.

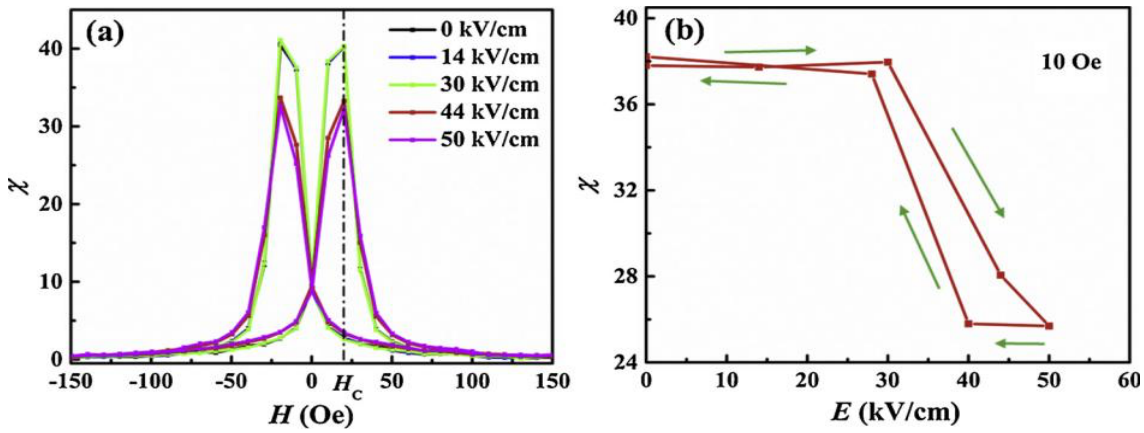

Fig. 4. (a) χ-H curves with different electric fields and (b) χ-E curve at 10 Oe of YIG/Pt/PLZST/Pt heterostructure